A cadmium(II)-based metal-organic framework for selective trace detection of nitroaniline isomers and photocatalytic degradation of methylene blue in neutral aqueous solution

Pengyan Wu [a], Yanhong Liu,[a] Yang Li,[a] Min Jiang,[a] Xiu-ling Li,[a] Yanhui Shi[a] and Jian Wang [a,*]

[a]*School of Chemistry and Chemical Engineering & Jiangsu Key Laboratory of Green Synthetic Chemistry for Functional Materials, Jiangsu Normal University, Xuzhou, Jiangsu, 221116, People's Republic of China*

Contents

1. X-ray Crystallography (Single-crystal diffraction) and Characterizations.

1.1 Figure S1 The coordination configuration of the Cd(1) and Cd(2) centre in Cd−**PDA**. The asymmetric mode: A: x, 1+y, z; B: 1.5-x, 0.5+y, 0.5-z.

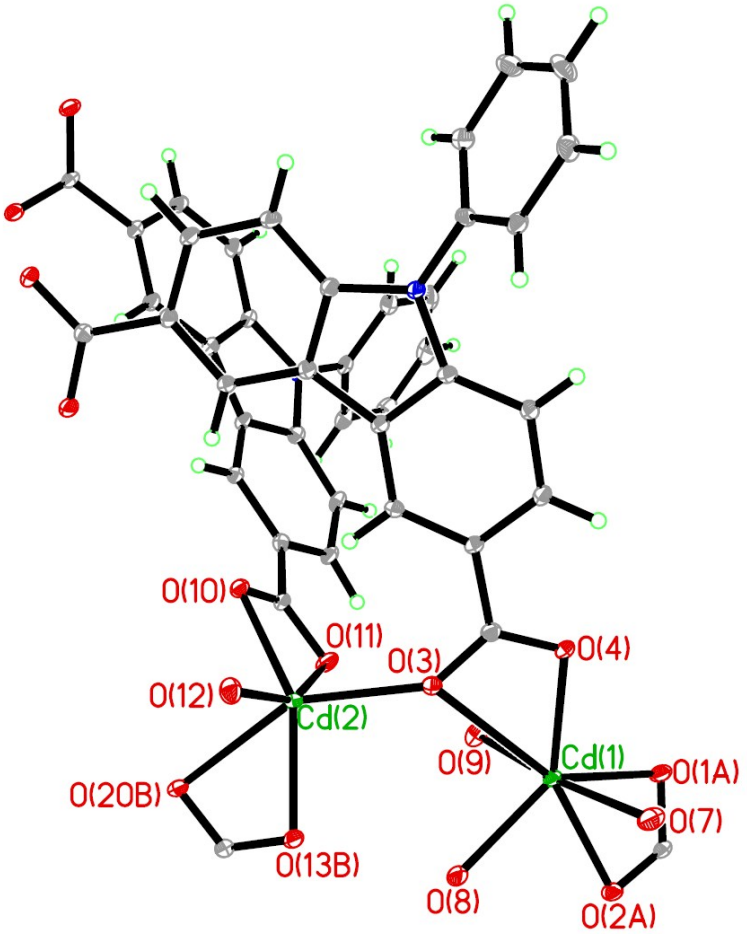

1.2 Selective bond distance (Å) and angle (°) in Cd−**PDA**.

Selective bond distance (Å): Cd(1)−O(4) 2.2403(2), Cd(1)−O(8) 2.263(2), Cd(1)−O(2A) 2.3171(2), Cd(1)−O(7) 2.3192(2), Cd(1)−O(9) 2.3299(2), Cd(1)−O(1A) 2.4537(2), Cd(2)−O(12) 2.1982(2), Cd(2)−O(13B) 2.2054(2), Cd(2)−O(3) 2.2387(2), Cd(2)−O(10) 2.2864(2), Cd(2)−O(11) 2.3872(2), Cd(2)−O(20B) 2.5549(2).

Selective bond angle (°): O(4)−Cd(1)−O(8) 124.18(7), O(4)−Cd(1)−O(2A) 149.93(6), O(8)−Cd(1)−O(2A) 82.22(7), O(4)−Cd(1)−O(7) 84.03(7), O(8)−Cd(1)−O(7) 93.03(8), O(2A)−Cd(1)−O(7) 80.06(6), O(4)−Cd(1)−O(9) 94.65(7), O(8)−Cd(1)−O(9) 94.13(8), O(2A)−Cd(1)−O(9) 97.64(6), O(7)−Cd(1)−O(9) 172.11(7), O(4)−Cd(1)−O(1A) 100.41(6), O(8)−Cd(1)−O(1A) 135.41(7), O(2A)−Cd(1)−O(1A) 54.83(6), O(7)−Cd(1)−O(1A) 90.93(6), O(9)−Cd(1)−O(1A) 81.65(6), O(12)−Cd(2)−O(13B) 97.91(7), O(12)−Cd(2)−O(3) 105.45(6), O(13B)−Cd(2)−O(3) 96.67(6), O(12)−Cd(2)−O(10) 101.31(6), O(13B)−Cd(2)−O(10) 139.63(6), O(3)−Cd(2)−O(10) 111.66(6), O(12)−Cd(2)−O(11) 157.45(7), O(13B)−Cd(2)−O(11) 101.15(6), O(3)−Cd(2)−O(11) 84.24(6), O(10)−Cd(2)−O(11) 56.18(6), O(12)−Cd(2)−O(20B) 94.39(6), O(13B)−Cd(2)−O(20B) 54.45(6), O(3)−Cd(2)−O(20B) 147.42(6), O(10)−Cd(2)−O(20B) 88.77(6).

1.3 Figure S2 PXRD patterns of the as-synthesized (red), the simulated from single X-ray crystal structure (black).

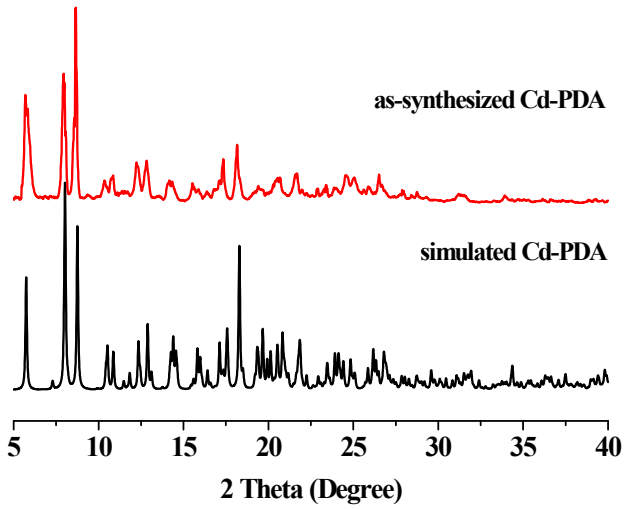

1.4 Figure S3 CO_2 adsorption/desorption isotherms of Cd−**PDA** at 195 K.

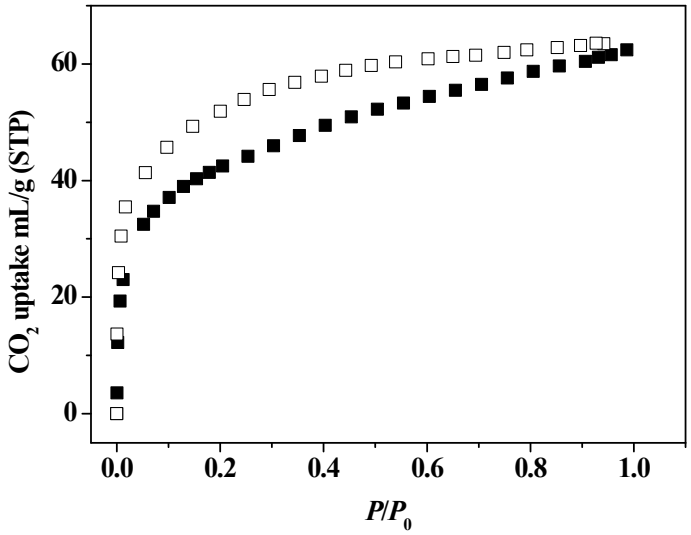

1.5 Figure S4 TGA traces of Cd−**PDA** ranging from room temperature to 500 °C.

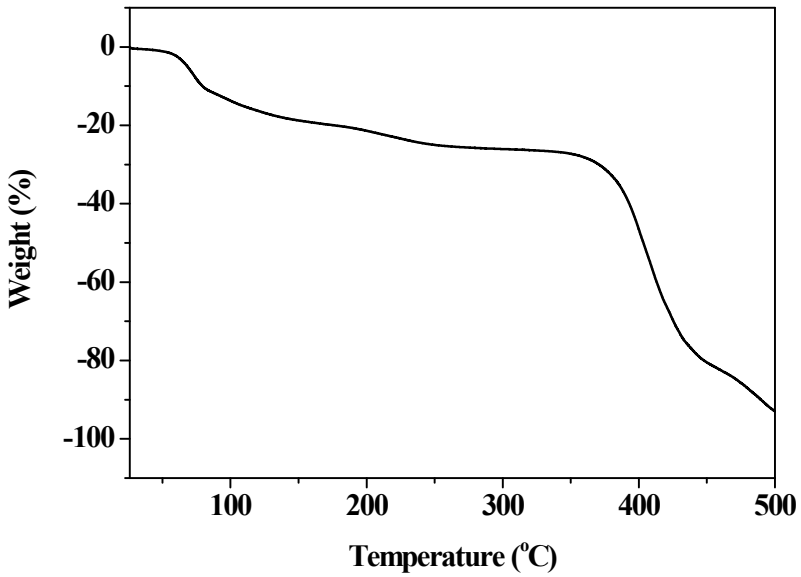

2. Studies on the nitro-explosives detection based on Cd−PDA.

2.1 Figure S5 The UV/vis absorption spectra for solid Cd−**PDA.**

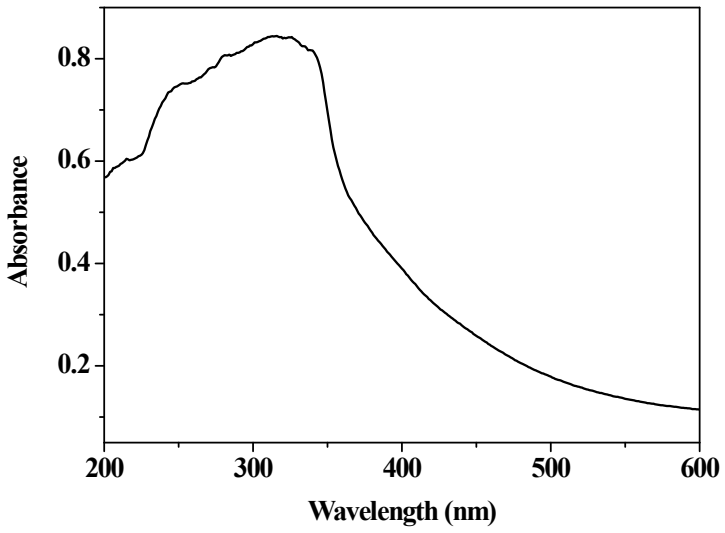

2.2 Figure S6 The Stern−Volmer plot of Cd−**PDA** quenched by *p*-NA ethanol solution, where I_0 and I are the fluorescence intensity before and after *p*-NA incorporation, respectively.

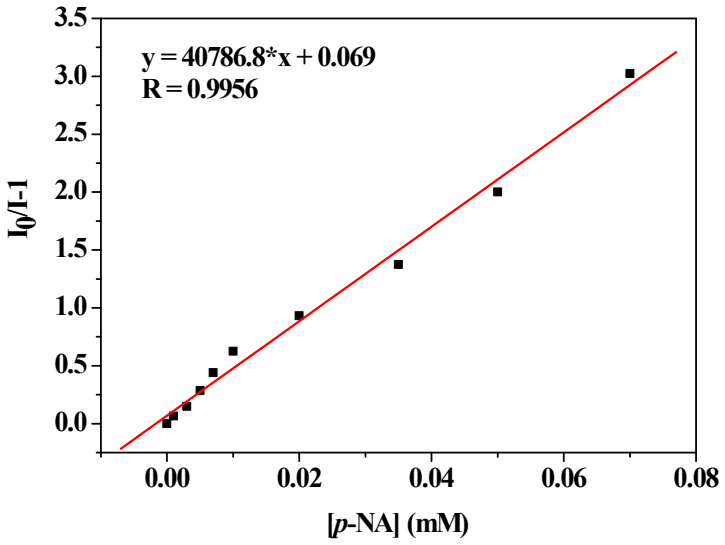

2.3 Figure S7 Families of various fluorescence spectra of Cd−**PDA** in ethanol solution upon the addition of 0.125 mM of different selected analytes.

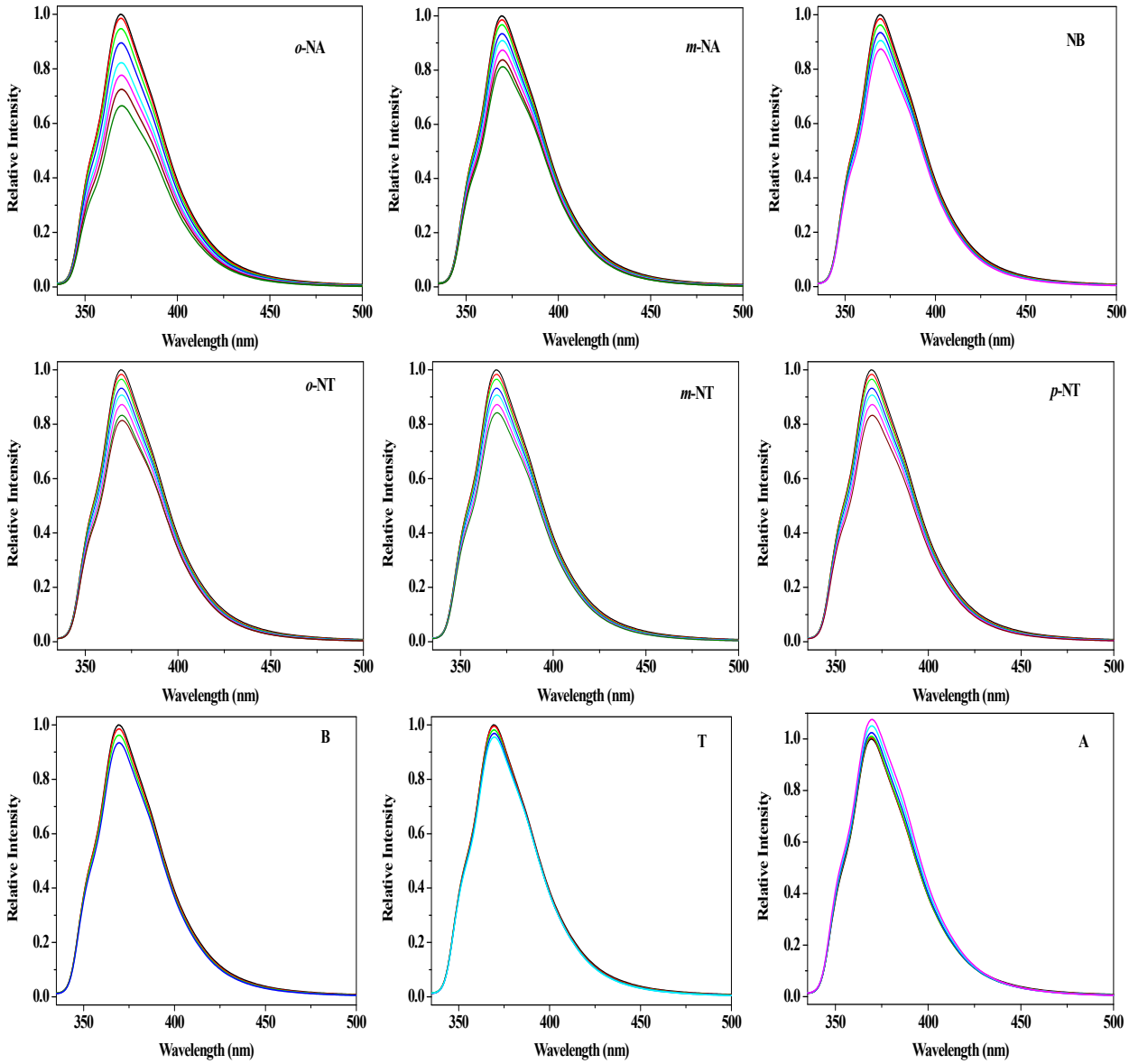

2.4 Figure S8 (Left) FT-IR spectra of *o*-NA (top), Cd–**PDA** impregnated with *o*-NA solution (middle) and Cd–**PDA** (bottom); (Right) FT-IR spectra of *m*-NA (top), Cd–**PDA** impregnated with *m*-NA solution (middle) and Cd–**PDA** (bottom).

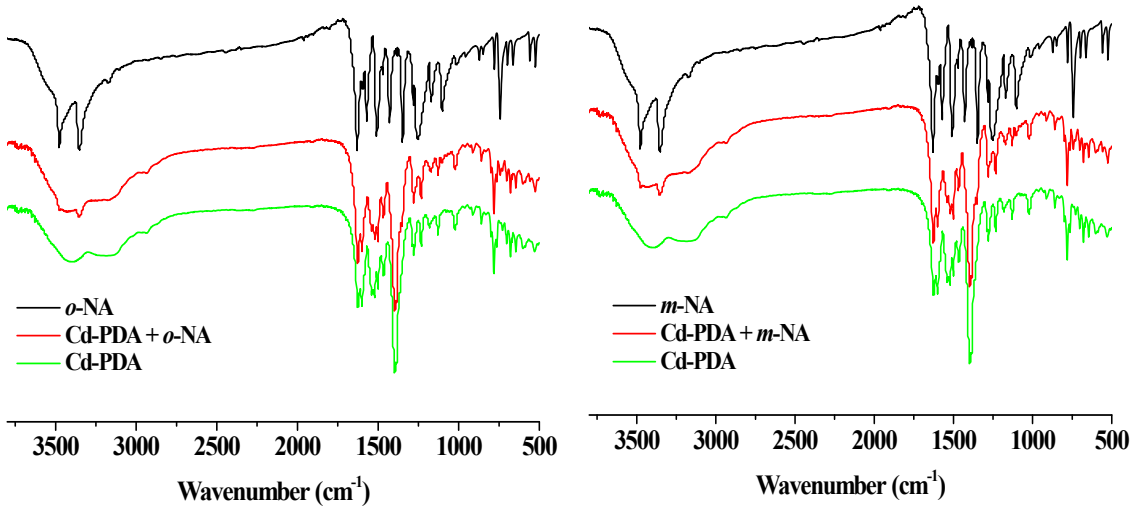

2.5 Figure S9 Representation of the interaction between Cd−**PDA** and *o*-NA (left) and *m*-NA (right) computed by molecular force field-based calculations.

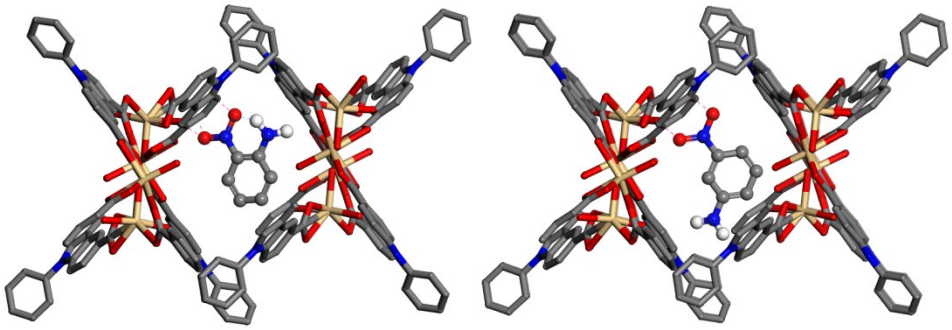

o-NA *m*-NA

3. Studies on the photodegradation of MB based on Cd−PDA.

3.1 Figure S10 The first-order plots for the photodegradation of MB using Cd−**PDA**.

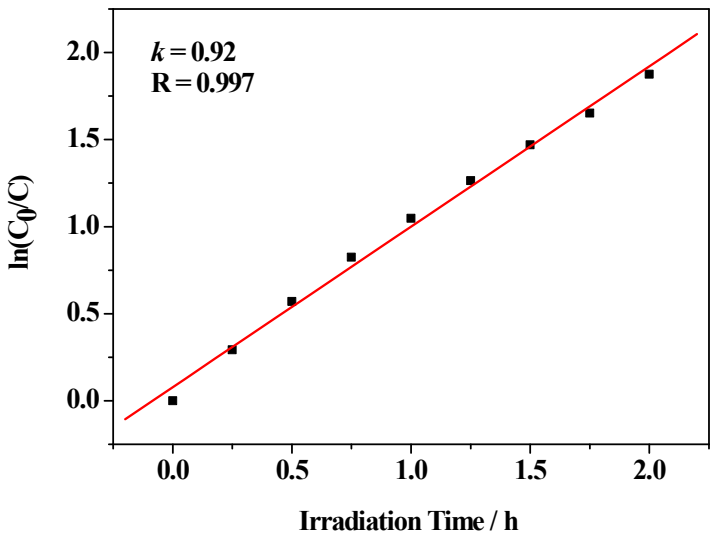

3.2 Figure S11 Recycling experiments employing Cd−**PDA** as a catalyst for the degradation of MB under Xe lamp irradiation.